Annals of Biomedical Engineering, Vol. 34, No. 4, April 2006 *(© 2006)* pp. 669–676
DOI: 10.1007/s10439-005-9053-9

Neurite Outgrowth is Directed by Schwann Cell Alignment in the Absence of Other Guidance Cues

DEANNA M. THOMPSON[1,3] and HELEN M. BUETTNER[1,2]

[1]Department of Chemical and Biochemical Engineering, 98 Brett Road, Piscataway, NJ, 08854; [2]Department of Biomedical Engineering, Rutgers, The State University of New Jersey, 98 Brett Road, Piscataway, NJ 08854; and [3]Current address: Department of Biomedical Engineering, Rensselaer Polytechnic Institute, Troy, NY

(Received 26 April 2005; accepted 28 July 2005; published online: 21 March 2006)

Abstract— Schwann cells enhance axonal regeneration following nerve injury in vivo and provide a favorable substrate for neurite outgrowth *in vitro*. However, much remains unknown about the nature of interactions that occur between Schwann cells and growing neurites. In this paper, we describe direct evidence of the ability of Schwann cell alignment alone to direct neurite outgrowth. Previously, we reported that laminin micropatterns can be used to align Schwann cells and thus create oriented Schwann cell monolayers. In the current study, dissociated rat spinal neurons were seeded onto oriented Schwann cell monolayers, whose alignment provided the only directional cue for growing neurites, and neurite alignment with the underlying Schwann cells was analyzed. The orientation of neurite outgrowth mimicked that of the Schwann cells. Associations observed between neurites and Schwann cells suggest that Schwann cells may guide neurite outgrowth through both topographical and molecular mechanisms. This work demonstrates that Schwann cell alignment can direct neurite outgrowth in the absence of other directional cues, and provides a new method for examining neuronal–Schwann cell interactions *in vitro*.

Keywords—Axonal regeneration, Nerve regeneration, Neurite guidance, Micropatterned laminin, Cell orientation, Coculture, Cell monolayer, Topography.

INTRODUCTION

Following injury, nerve regeneration is possible if the neuronal cell bodies are intact and the growing axons are provided with the proper microenvironment. Guidance cues that direct axonal regrowth along an appropriate spatial pathway are an important feature of the regeneration environment. A number of acellular cues have been shown to guide neurite outgrowth, including substrate bound pathways,[15,21,22,23,30] surface topography,[13,16,18,26,27,36] and gradients of diffusible factors.[31,32] Increasingly, cellular cues are also being considered in tissue engineering approaches to nerve regeneration. Key among these are Schwann cells, glial cells of the peripheral nervous system whose presence in nerve grafts enhances the regeneration of both peripheral[20,38] and central[7,9] nerves.

Schwann cells provide a rich and supportive environment for neurite outgrowth through the release of neurotrophic factors, expression of cell surface ligands, and synthesis of extracellular matrix (ECM).[8,9,19] A variety of regeneration-promoting cell adhesion molecules are expressed on the surface of Schwann cells, including heparin-sulfate proteoglycan (HSPG),[10] neural cell adhesion molecule (NCAM), and L1.[24] The ECM components produced by Schwann cells are expressed on their surface as well as deposited and organized into a basal lamina.[3,8,14] In addition, Schwann cells can produce inhibitory molecules such as myelin-associated glycoprotein (MAG) that may balance the effects of permissive factors by inhibiting outgrowth and branching.[29]

The directional influence of Schwann cell orientation on neurite outgrowth has been suggested by axonal regeneration parallel to aligned Schwann cells in injured peripheral[20] and central[5,6] nerve tissue as well as in oriented collagen gels,[17] oriented fibronectin mats,[37] microtextured polymeric substrates, The focus of the work presented here was to test the ability of Schwann cell orientation alone to guide neurite outgrowth. To achieve this, we used Schwann cell monolayers aligned on a planar substrate of lithographically patterned laminin, as we have previously described.[34] Dissociated rat spinal neurons were seeded onto the monolayers, and neurite outgrowth orientation was compared quantitatively with the underlying Schwann cell orientation. Qualitative features of neurite–Schwann cell interactions were also observed. Our results demonstrate an unambiguous effect of Schwann cell alignment on directional neurite outgrowth and suggest that guidance occurs through more than one mechanism.

Address correspondence to Helen M. Buettner, PhD Department of Biomedical Engineering, Rutgers, The State University of New Jersey, 98 Brett Road, Piscataway, NJ 08854. Electronic mail: buettner@rci.rutgers.edu

MATERIALS AND METHODS

Oriented Schwann Cell Monolayers

The preparation of oriented Schwann cell monolayers has been described in detail by Thompson and Buettner[34] and is summarized only briefly here. Substrates for orienting the Schwann cells were created by lithographically micropatterning no. 1, 18 mm round glass coverslips with alternating 20-μm wide laminin stripes and 10-μm wide bovine serum albumin (BSA) stripes. Schwann cells isolated from neonatal rat sciatic nerves (a kind gift from J. Salzer, NYU) were expanded in a serum-containing growth medium and treated with complement-mediated cell lysis to ensure purity, which was confirmed by staining with FITC-conjugated anti-S100. Cells were seeded onto the micropatterned coverslips at a density of 1.32×10^4 cells/cm^2 in serum-free medium and incubated at 37°C and 7% CO_2 to permit cell alignment with the pattern. At 20–24 h post-seeding, the medium was changed to a serum-containing medium to promote cell proliferation. Cells were allowed to proliferate to confluency, which was reached at 5 to 6 days post-seeding. This procedure yielded a monolayer of Schwann cells aligned with the underlying pattern. Control monolayers were prepared by seeding Schwann cells onto uniform laminin substrates, which resulted in a monolayer of randomly oriented cells.

Neuronal Cocultures

Spinal ganglia were dissected from P0–P2 neonatal rat pups and rinsed in HBSS to remove extraneous tissue. The ganglia were pelleted, then resuspended in 1 ml of 1 mg/ml collagenase (Boehringer Mannheim, Indianapolis IN) and 0.1% trypsin (Fisher Scientific) in HBSS. After incubation at 37°C for 50 min, the ganglia were pelleted and resuspended in 1 ml of 0.25% trypsin solution for 10 min at 37°C. The enzymatic digestion was neutralized by adding serum-containing medium. The serum-containing medium was removed and the cells were resuspended in warmed serum-free neuronal medium consisting of 1:1 v/v DMEM/Ham's F-12 media, 10 mg/ml glucose (Sigma Chemical), 20 μl/ml N3, 2 mM L-glutamine, 0.1% BSA, 1 × MEM vitamins (Life Technologies), 50 U P/S, 6.25 ng/ml ITS+ premix (Fisher Scientific) and 12 ng/ml 7.5NGF (Fisher Scientific). N3 consisted of 5 ml of N2 supplement (Fisher Scientific), 12.5 μl of 200 μg/ml of T3 (Sigma Chemical), 250 μl of 0.625 mg/ml of ITS and 10 μl of 2 mg/ml corticosterone (Sigma Chemical). The dissociation was completed by gently triturating 10–20 times with a sterile, flame polished, reduced bore glass pipette. Dissociated neurons were plated at 2×10^4 cells/cm^2 onto oriented Schwann cell monolayers and onto three control substrates: (a) unoriented Schwann cell monolayers, (b) micropatterned laminin, and (c) uniform laminin. After an 18 h incubation at 37°C in 7% CO_2, the cocultures were fixed in 4% formaldehyde (Fisher Scientific) for 20 min and gently rinsed twice in HBSS.

Immunofluorescence

Fixed samples were permeabilized in 0.1% Triton X-100 (Fisher Scientific) and blocked with 10% heat inactivated fetal goat serum (FGS; Sigma Chemical) in PBS for 1 h, gently rinsed in PBS, then blocked overnight with 10% FGS diluted in HBSS at 4°C. The next day, the samples were treated with two primary antibodies, monoclonal anti-neurofilament 200 (Sigma Chemical) and monoclonal anti-neurofilament 160 (Chemicon Inc., Temecula CA), both diluted 1:100 in HBSS, and incubated overnight at 4°C. The treated samples were rinsed with HBSS and incubated with a secondary antibody, FITC-conjugated goat anti-mouse IgG (Sigma Chemical), for 1 h at room temperature, wrapped in foil to prevent exposure to light. After rinsing with HBSS to remove unbound secondary antibody, the samples were incubated for 30 min in ethidium bromide (EtBr) diluted 1:2000, then rinsed in HBSS. Samples were covered with anti-fade solution and wrapped with foil to prevent photobleaching prior to imaging.

Image Analysis

Stained samples were inverted, mounted onto a glass slide, sealed with a 1:1:1 mixture of vaseline, lanolin, and parafinn as previously described,[30] and imaged on a Zeiss LSM 410 confocal microscope in fluorescence mode. Orientation distributions, neuronal characteristics, and Schwann cell spacing were measured using a 20× objective in fluorescence mode. Images for topographical analysis were obtained using a 40× objective. Neuronal staining with FITC-conjugated anti-neurofilament (green) and nuclear staining with EtBr (red) was visualized at excitation/emission wavelengths of 488/512 and 568/605 nm, respectively. Images were imported into NIH Image 1.61 (National Institutes of Health, USA) for analysis as described below.

Neuronal Characteristics

Neurite outgrowth orientation was determined for each neuron in each image by tracing the perimeter of the neurite arbor and fitting it to an ellipse of the same area. The orientation was measured as the angle between the major axis of the ellipse and the vertical axis of the image plane. Orientation angles were subsequently converted to yield a mean direction of 0°. The aspect ratio of the outgrowth area was calculated as the ratio of the major axis, α, to the minor axis, β. The neuronal cell body was manually traced to measure its area and the number of primary neurites projecting from each cell body were counted and recorded.

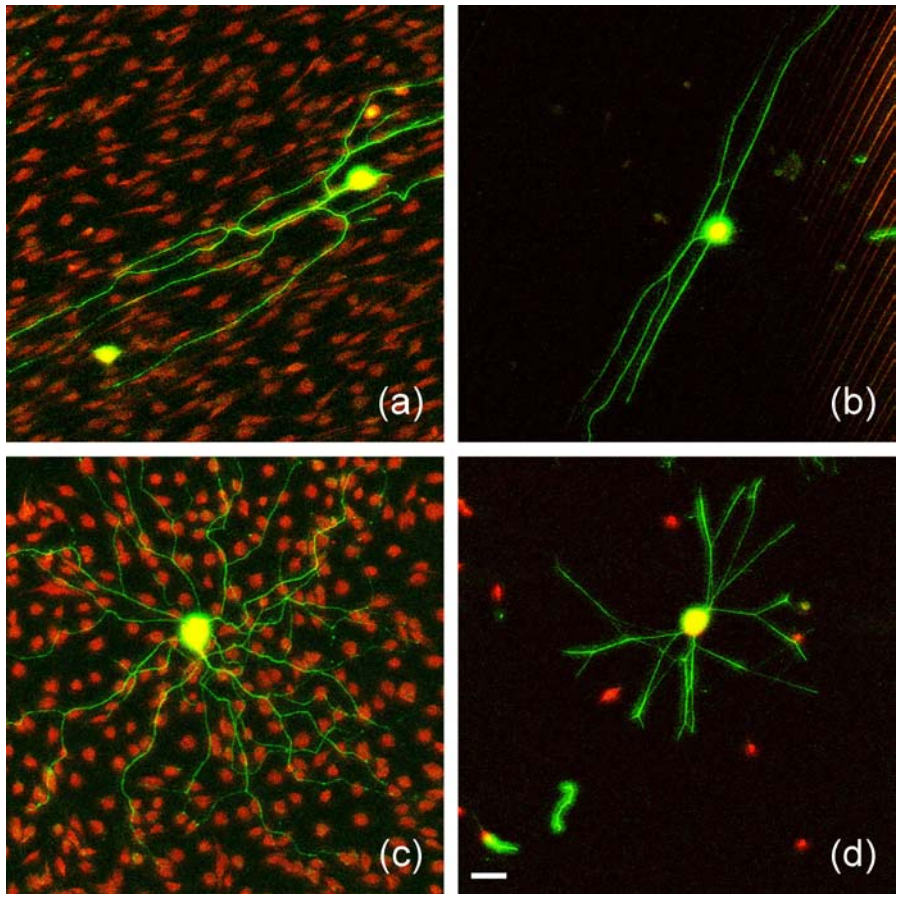

Figure 1. Neurite outgrowth on (a) aligned Schwann cell monolayer, (b) micropatterned laminin, (c) unaligned Schwann cell monolayer, and (d) uniform laminin. *Bar* = 50 μm.

An estimate of the neurite density was obtained by measuring the total fluorescence area of a given neuron, A_{neuron}, and subtracting the cell body area, $A_{\text{cell body}}$, from this to obtain the fluorescence area contributed by the neurites alone

$$A_{\text{neurite}} = A_{\text{neuron}} - A_{\text{cell body}} \quad (1)$$

A_{neurite} was divided by the number of primary neurites extending from the neuronal cell body to obtain the neurite area per primary neurite. Duplicate samples were analyzed at each experimental condition and the results averaged. Mean neuronal characteristics were compared using a one-way ANOVA Least Significant Difference (LSD) post hoc test with significance determined at $P < 0.05$.

Schwann Cell Monolayer Orientation and Spacing

The orientation of individual Schwann cells in each image was determined from the orientation of their nuclei.[34] Images were inverted, thresholded and the area and orientation of each nucleus was measured. Schwann cell orientation angles were transformed by the same conversion applied to the neurite orientation angles to maintain the angular relationship between the two data sets. Although neuronal nuclei were also stained by EtBr and therefore included in this measurement, neurons accounted for $< 1\%$ of the nuclei. Schwann cell nucleus spacing was analyzed for four representative monolayers by measuring the center-to-center distance between nuclei parallel and perpendicular to their mean direction of alignment.

Schwann Cell Topography

To determine the Schwann nucleus height, representative Schwann cell monolayers were optically sectioned at successive 1-μm intervals from the coverslip surface. Each image in the stack was inverted and thresholded to identify the individual nuclei. In a given image, each nucleus was fit to an ellipse of the same area, and the minor axes of the ellipses were averaged to obtain an estimate of the mean minimum nucleus width in that image. The mean nucleus height was then obtained by plotting the mean minimum nucleus width as a function of distance from the coverslip.

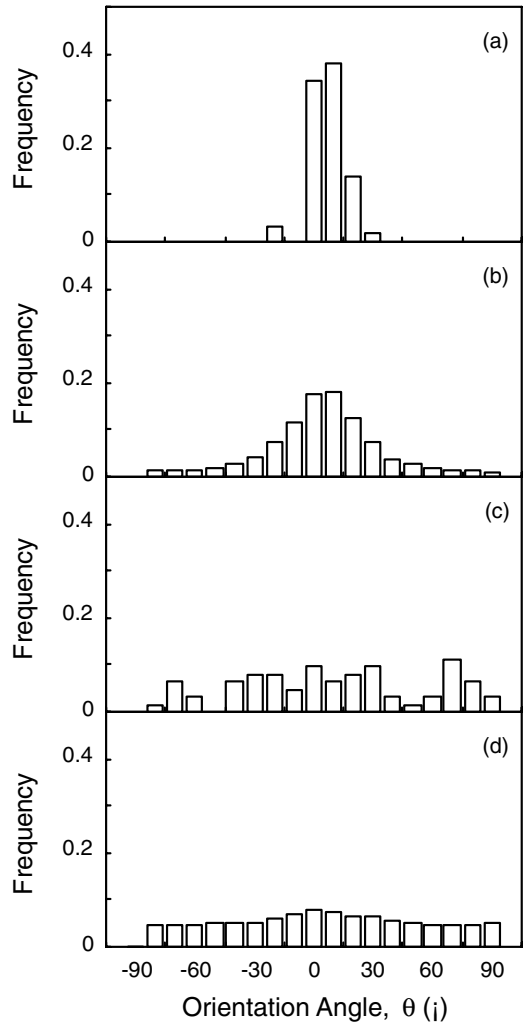

Figure 2. Orientation frequency distributions. (a) Neurites growing on aligned Schwann cells exhibited the same mean direction as (b) the underlying Schwann cells. (c) Neurites growing on unoriented Schwann cell monolayers mimicked (d) the uniform orientation distribution of the Schwann cells.

RESULTS

Neurite Alignment by Schwann Cell Monolayers

As illustrated in Fig. 1(a), neurites grown on oriented Schwann cell monolayers aligned with the underlying Schwann cells. The degree of alignment was similar to that observed for neurites grown on micropatterned laminin substrates, shown in Fig. 1(b). In contrast, neurites grown on unoriented Schwann cell monolayers or on uniform laminin substrates extended radially about the cell body (Figs. 1(a) and 1(d)).

Neurite and Schwann cell alignment are compared quantitatively in Fig. 2 in terms of the distribution of orientation angles. On aligned Schwann cell monolayers, the mean neurite orientation coincided with Schwann cell orientation, as shown in Figs. 2(a) and 2(b). The lack of orientation bias in Schwann cell monolayers formed on uniform laminin substrates, characterized by a flat frequency distribution, was reflected in the neurite orientation (Figs. 2(c) and 2(d)). The alignment of neurite outgrowth on oriented Schwann cell monolayers was similar to that on micropatterned laminin surfaces (not shown). Eighty seven percent of the neurites on the Schwann cell monolayer were oriented to within 10° of the mean ($|\theta| \leq 10°$) neurite alignment on the laminin micropattern was 94%.

Neurite–Schwann Cell Interactions

Four distinct interactions between neurites and Schwann cells were observed in coculture experiments, as illustrated in Fig. 3. Neurites were commonly seen on top of Schwann cell nuclei (boxes 1–3), between two adjacent nuclei (box 4), and around the base of a single nucleus (boxes 6–7). Occasionally, a neurite branched at the base of a nucleus, with each branch extending around it in a different direction (box 5). As summarized in Fig. 4, topographical analysis of the Schwann cell monolayer revealed, on average, 11-μm high nuclei. These occurred at a mean interval of 67.9 μm (SE = 1.6 μm, $n = 520$) in the direction of the micropattern and 37.8 μm (SE = 1.1 μm, $n = 662$) perpendicular to the micropattern. The maximum nucleus dimensions parallel to the plane of the coverslip averaged 9.2 ± 2.6 μm wide by 19.0 ± 4.3 μm long.

Neuronal Characteristics

Characteristics of the neurons on oriented Schwann cell monolayers are compared in Table 1 with the same characteristics on the three control substrates. The statistical significance of the difference between mean values for the different substrates is summarized in Table 2. Neurons on Schwann cell monolayers produced more primary neurites than neurons on acellular laminin substrates. However, the number of primaries was unaffected by substrate alignment. Cell body area was larger on unaligned Schwann cell substrates, but did not vary significantly between the other substrates. The total area of neurite fluorescence per primary neurite was greatest on aligned Schwann cells, as shown in Fig. 5, decreasing signficantly on both laminin and micropatterned laminin. The major axis of the neurite arbor was similar in all cases, but substrate alignment restricted growth in the perpendicular direction.

DISCUSSION

In previous work, we demonstrated that micropatterned laminin substrates can be utilized to control Schwann cell orientation[33] and to create oriented Schwann cell monolayers.[34] In the current work, we have used oriented Schwann cell monolayers to provide direct evidence that Schwann cell alignment provides an effective guidance cue for neurite outgrowth in the absence of other directional cues, and

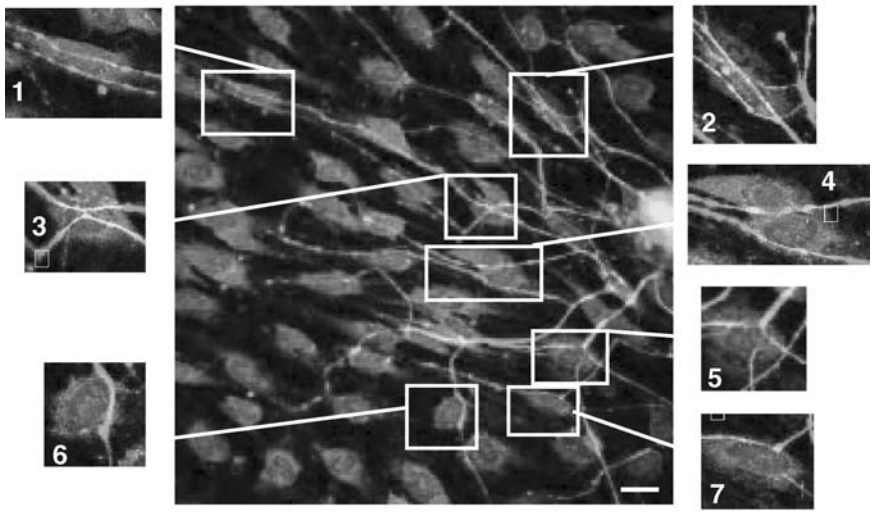

Figure 3. Neurite extension on aligned Schwann cell monolayers occurred: (1) over the Schwann cell nucleus (boxes 1–3), (2) between two nuclei (box 4), (3) by branching at the base of the nucleus (box 5), and 4) around the nucleus (boxes 6–7). Bar = 10 μm.

that it may do so *via* more than one mechanism. Unlike other systems in which Schwann cells have been aligned using surface topography, which may also serve to guide growing neurites, the only directional information available to neurites in our system is due to the Schwann cell monolayer. Thus, our approach makes it possible to isolate and evaluate the neurite response to Schwann cell alignment without the complicating influence of unrelated topographical cues from the underlying substrate.

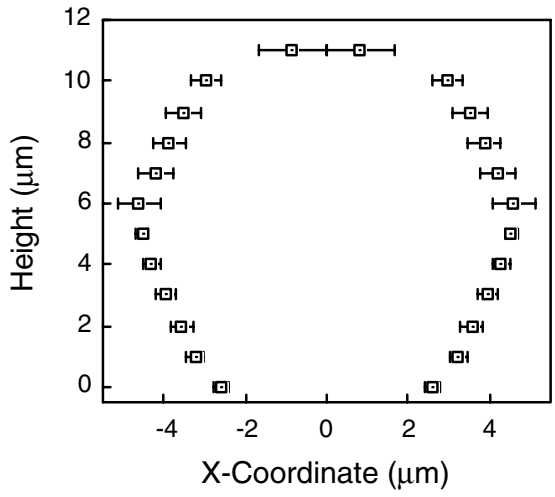

Figure 4. Mean cross-section of the Schwann cell nucleus perpendicular to the culture surface, obtained by optically sectioning representative oriented Schwann cell monolayers at successive 1-μm intervals above the culture surface using confocal microscopy and fitting the individual nucleus cross-sections in each image to a same-area ellipse. The minor axes of the nuclei in a given image plane were averaged to obtain the mean minor axis, which is plotted here (centered at zero) as a function of height above the culture surface.

The alignment of neurite outgrowth with oriented Schwann cells was apparent both qualitatively and quantitatively. The orientation frequency distributions measured for neurite outgrowth on both oriented and unoriented Schwann cells mirrored those of the Schwann cells. Although the distribution of Schwann cell orientation seen in Fig. 2(a) is broader than the distribution of neurite orientation, this reflects the fact that Schwann cell nuclei are much shorter than the outgrowth of a neuron. If neurite orientation were characterized for segments of single neurites similar in length to the Schwann cell nucleus, greater variability would be observed in neurite orientation as well. Measuring neurite orientation in terms of the entire neurite arbor of a neuron averages out some of the "noise" in the distribution.

Outgrowth orientation on Schwann cell monolayers was similar to that seen on acellular micropatterned laminin surfaces, where neurite outgrowth preferentially elongates parallel to the laminin stripe. However, unlike micropatterned laminin, the Schwann cell monolayer has a micron scale topography due to the three-dimensional nature of cell morphology. Our results suggest that this cellular topography plays a role in neurite guidance. Of the neurite–Schwann cell associations we observed, growth around and between nuclei as well as branching at the base of a nucleus may be indicative of a contact guidance mechanism, with the nucleus serving as a physical cue. The Schwann cell monolayer on which neurites were grown was "bumpy," consisting of flat cytoplasmic regions punctuated by 11-μm high nuclei. Although measurement of the height of the extranuclear cytoplasmic region was beyond the scope of this work, the thickness of fibroblast lamellipodia on glass cov-

Table 1. Neuronal characteristics.

Substrate	Primary neurites/cell ± SE	Cell body area ± SE (μm^2)	Neurite area/primary ± SE (μm^2)	Minor axis of neurite arbor, β, ± SE (μm)	Aspect ratio of neurite arbor, α/β
Aligned Schwann cells	4.05 ± 0.24	1252.2 ± 30.8	2711.4 ± 307.0	235.5 ± 13.5	3.0
Unaligned Schwann cells	4.57 ± 0.24	1430.8 ± 36.5	2145.8 ± 163.0	351.0 ± 26.4	1.6
Micropatterned laminin	3.13 ± 0.16	1257.8 ± 31.0	1692.5 ± 220.8	86.1 ± 7.4	8.3
Uniform laminin	3.36 ± 0.17	1199.6 ± 32.7	1624.2 ± 158.3	291.1 ± 24.3	1.6

erslips has been measured at less than 200 nm.[1] Assuming that the Schwann cell plasma membrane flattens to a similar degree, the nucleus presents an obstacle on the order of 10 μm high to a neurite growing on the surrounding plasma membrane. Physical features as much as two–three orders of magnitude smaller than this in various substrata have been shown to guide neurite outgrowth.[11,13,16–18,27,28,35]

In addition to neurites circumnavigating the nucleus, we frequently observed neurites exended over the top the nucleus, which cannot be explained by a contact guidance mechanism. Rather this behavior points toward the influence of specific molecular cues on the Schwann cell surface favorable enough to direct the migrating neurite over the "hill" represented by the nucleus. Candidate molecules are suggested by studies that have identified regions of permissive surface molecules on the Schwann cell surface in culture and in vivo. Cornbrooks *et al*. (1983) found a "spotty" pattern of laminin staining on Schwann cells *in vitro* and in vivo, with an in vivo localization believed to correspond to the Schwann cell nuclear region.[14] Carey *et al*. (1993) showed heparin sulfate proteoglycans (HSPG) expressed on the surface of Schwann cells in small 100–200 nm diameter regions,[10] and Martini *et al*. (1994) reported L1 and NCAM at sites of contact with neurites.[24] Further suggestion that one or more of these molecules may provide directional information on the Schwann cell surface is provided Biran *et al*. (2003), who found linear arrays of laminin, fibronectin, NCAM, and chondroitin sulfate proteoglycan (CSPG) on the surface of aligned astrocytes, central nervous system glial cells that also guide neurite outgrowth.[4] While laminin and NCAM were concentrated on top of the cell, fibronectin and CSPG appeared between adjacent astrocytes. If similar distributions occur on Schwann cells, it is possible that molecular cues not only guide growing neurites over the top of the Schwann cell nucleus but also around its base.

Schwann cells promoted a more complex neurite morphology than acellular laminin surfaces. Neurons on aligned and unaligned Schwann cells displayed more primary neurites than neurons on the corresponding laminin surfaces. Neurite branching also appeared to increase in the presence of Schwann cells, based on measurements of the total neurite area per primary neurite. This parameter reflects an increase in neurite "mass" emanating from the primary neurites of neurons on Schwann cells relative to laminin substrates, which could result from either an increase in neurite extension or branching. However, neurite extension did not differ significantly between the different substrates, suggesting that the effect was due to branching. These results are somewhat in contrast to the findings of Clark *et al*.[12] that neurons on uniform laminin substrates exhibit a multipolar, branched morphology while neurons on mi-

Table 2. Statistically significant differences in mean neuronal characteristics[a].

	Unaligned Schwann cells	Micropatterned laminin	Uniform laminin
Aligned Schwann cells	C, M	M, N, P	M, N, P
Unaligned Schwann cells	—	M, C, P	C, N, P
Micropatterned laminin		—	NS*

[a]Entries indicate characteristics for which a significant difference occurred between the two conditions, as evaluated by a one-way ANOVA LSD post hoc test. Abbreviations: C: Cell body area, M: Minor axis of neurite arbor,* N: Neurite area/primary, P: Primary neurites/neuron, NS: No significant differences

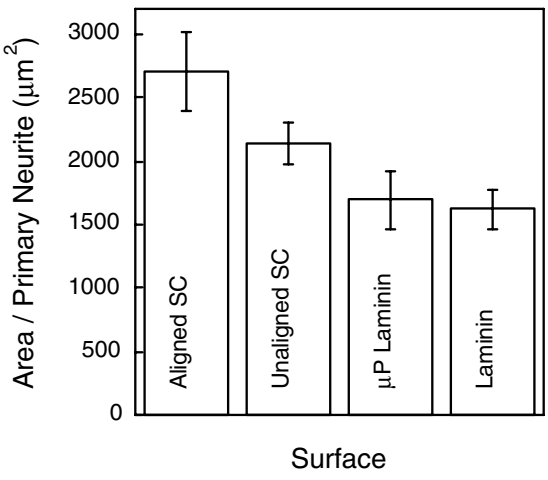

Figure 5. The mean outgrowth area per primary neurite was significantly greater on cellular substrates than on the laminin substrates.

cropatterned laminin adopt a bipolar, unbranched morphology, suggesting that the lateral constraints placed on neurite outgrowth by the micropattern inhibited the development of a complex morphology.[9] In our experiments, neurons developed multipolar morphology on all surfaces, and neither the number of primary neurites nor branching behavior was signficantly affected by the presence or absence of substrate orientation.

In summary, we have demonstrated that Schwann cell alignment directs neurite outgrowth in the absence of other directional information. Guidance is likely influenced by both the topography of the Schwann cell monolayer and molecules expressed on the Schwann cell surface. The new coculture system we have described makes it possible to further elucidate the contributions of these guidance cues to axonal regeneration and to investigate other Schwann cell–neuronal interactions that may be important in successful regeneration, with the ultimate goal of providing mechanistic insight to guide the development of clinically relevant strategies for nerve repair.

ACKNOWLEDGMENTS

We thank Wise Young and Kai Liu for helpful discussions, use of laboratory facilities and technical assistance; Robin Davis and Crista Adamson for discussions concerning antibody selection; Surya Mallapragda and Greg Rutkowski for discussions about dissociation techniques. This work was supported by the Charles and Johanna Busch Memorial Fund, the Rutgers-UMDNJ Biotechnology Training Program, a Johnson & Johnson Research Fellowship (DMT) and an AAUW Selected Professions Dissertation Fellowship (DMT).

REFERENCES

[1]Abraham, V. C., V. Krishnamurthi, D. L. Taylor, and F. Lanni. The actin-based nanomachine at the leading edge of migrating cells. *Biophys. J.* 77:1721–1732, 1999.

[2]Ahmed, Z., and R. A. Brown. Adhesion, alignment, and migration of cultured Schwann cells on ultrathin fibronectin fibres. *Cell Motil. Cytoskeleton* 42:331–343, 1999.

[3]Ard, M. D., R. P. Bunge, and M. B. Bunge. Comparison of the Schwann cell surface and Schwann cell extracellular matrix as promoters of neurite growth. *J. Neurocytol.* 16:539–555, 1987.

[4]Biran, R., M. D. Noble, and P. A. Tresco. Directed nerve outgrowth is enhanced by engineered glial substrates. *Exp. Neurol.* 184:141–152, 2003.

[5]Brook, G. A., J. M. Lawrence, B. Shah, and G. Raisman. Extrusion transplantation of Schwann cells into the adult rat thalamus induces directional host axon growth. *Exp. Neurol.*. 126:31–43, 1994.

[6]Brook, G. A., D. Plate, R. Franzen, D. Martin, G. Moonen, J. Schoenen, A. B. Schmitt, J. Noth, and W. Nacimiento. Spontaneous longitudinally orientated axonal regeneration is associated with the Schwann cell framework within the lesion site following spinal cord compression injury of the rat. *J. Neurosci. Res.* 53:51–65, 1998.

[7]Bunge, M. B., and D. D. Pearse. Transplantation strategies to promote repair of the injured spinal cord. *J. Rehabil. Res. Dev.* 40(4 Suppl 1):55–62, 2003.

[8]Bunge, R. P. Tissue culture observations relevant to the study of axon-Schwann cell interactions during peripheral nerve development and repair. *J. Exp. Biol.* 132:21–34, 1987.

[9]Bunge, R. P. The role of the Schwann cell in trophic support and regeneration. *J. Neurol.* 242:S19–S21, 1994.

[10]Carey, D. J., R. C. Stahl, V. K. Asundi, and B. Tucker. Processing and subcellular distribution of the Schwann cell lipid-anchored heparan sulfate proteoglycan and identification as glypican. *Exp. Cell Res.* 208:10–18, 1993.

[11]Ceballos, D., X. Navarro, N. Dubey, G. Wendelschafer-Crabb, W. R. Kennedy, and R. T. Tranquillo. Magnetically aligned collagen gel filling a collagen nerve guide improves peripheral nerve regeneration. *Exp. Neurol.* 158:290–300 1999.

[12]Clark, P., S. Britland, and P. Connolly. Growth cone guidance and neuron morphology on micropatterned laminin surfaces. *J. Cell Sci.* 105(Pt 1):203–212, 1993.

[13]Clark, P., P. Connolly, A. S. Curtis, J. A. Dow, and C. D. Wilkinson. Cell guidance by ultrafine topography in vitro. *J. Cell Sci.* 99(Pt 1):73–77, 1991.

[14]Cornbrooks, C. J., D. J. Carey, J. A. McDonald, R. Timpl, and R. P. Bunge. In vivo and in vitro observations on laminin production by Schwann cells. *Proc. Natl. Acad. Sci. USA* 80:3850–3854, 1983.

[15]Dertinger, S. K., X. Jiang, Z. Li, V. N. Murthy, and G. M. Whitesides. Gradients of substrate-bound laminin orient axonal specification of neurons. *Proc. Natl. Acad. Sci. USA* 99:12542–12547, 2002.

[16]Dowell-Mesfin, N. M., M.-A. Abdul-Karim, A. M. P. Turner, S. Schanz,H. G. Craighead, B. Roysam, J. N. Turner, and W. Shain. Topographically modified surfaces affect orientation and growth of hippocampal neurons. *J. Neural Eng.* 1:78–90, 2004.

[17]Dubey, N., P. C. Letourneau, and R. T. Tranquillo. Guided neurite elongation and schwann cell invasion into magnetically aligned collagen in simulated peripheral nerve regeneration. *Exp. Neurol.* 158:338–350, 1999.

[18]Dunn, G. A., and T. Ebendal. Contact guidance on oriented collagen gels. *Exp. Cell Res.* 111:475–479, 1978.

[19]Fawcett, J. W., and R. J. Keynes. Peripheral nerve regeneration. *Annu. Rev. Neurosci.* 13:43–60, 1990.

[20]Guenard, V., N. Kleitman, T. K. Morrissey, R. P. Bunge, and P. Aebischer. Syngeneic Schwann cells derived from adult nerves seeded in semipermeable guidance channels enhance peripheral nerve regeneration. *J. Neurosci.* 12:3310–3320, 1992.

[21]Gundersen, R. W. Guidance of sensory neurites and growth cones to patterned substrata of laminin and fibronectin in vitro. *Dev. Biol.* 121:423–431, 1987.

[22]Hammmerback, J. A., J. B. McCarthy, S. L. Palm, L. T. Furcht, and P. C. Letourneau. Growth cone guidance by substrate bound pathways is correlated with neuron-to-pathway adhesivity. *Dev. Biol.* 126:29–39, 1988.

[23]Letourneau, P. C. Cell-to-substratum adhesion and guidance of axonal elongation. *Dev. Biol.* 44:92–101, 1975.

[24]Martini, R., Y. Xin, and M. Schachner. Restricted localization of L1 and N-CAM at sites of contact between Schwann cells and neurites in culture. *Glia* 10:70–74, 1994.

[25]Miller, C., S. Jeftinija, and S. Mallapragada. Micropatterned Schwann cell-seeded biodegradable polymer substrates significantly enhance neurite alignment and outgrowth. *Tissue Eng.* 7:705–715, 2001.

[26]Miller, C., S. Jeftinija, and S. Mallapragada. Synergistic effects of physical and chemical guidance cues on neurite alignment

and outgrowth on biodegradable polymer substrates. *Tissue Eng*. 8:367–378, 2002.

[27]Rajnicek, A., S. Britland, and C. McCaig. Contact guidance of CNS neurites on grooved quartz: Influence of groove dimensions, neuronal age and cell type. *J. Cell Sci*. 110(Pt 23):2905–2913, 1997.

[28]Rangappa, N., A. Romero, K. D. Nelson, R. C. Eberhart, and G. M. Smith. Laminin-coated poly(L-lactide) filaments induce robust neurite growth while providing directional orientation. *J. Biomed. Mater. Res*. 51:625–634, 2000.

[29]Shen, Y. J., M. E. DeBellard, J. L. Salzer, J. Roder, and M. T. Filbin. Myelin-associated glycoprotein in myelin and expressed by Schwann cells inhibits axonal regeneration and branching. *Mol. Cell Neurosci*. 12:79–91, 1998.

[30]Tai, H. C., and H. M. Buettner. Neurite outgrowth and growth cone morphology on micropatterned surfaces. *Biotechnol. Prog*. 14:364–370, 1998.

[31]Tessier-Lavigne, M. Axon guidance by diffusible repellants and attractants. *Curr. Opin. Genet. Dev*. 4:596–601, 1994.

[32]Tessier-Lavigne, M., and M. Placzek. Target attraction: Are developing axons guided by chemotropism? *Trends Neurosci*. 14:303–310, 1991.

[33]Thompson, D. M., and H. M. Buettner. Schwann cell response to micropatterned laminin surfaces. *Tissue Eng*. 7:247–265,2001.

[34]Thompson, D. M., and H. M. Buettner. Oriented Schwann Cell Monolayers for Directed Neurite Outgrowth. *Ann. Biomed. Eng*. 32:1120–1130, 2004.

[35]Verdu, E., R. O. Labrador, F. J. Rodriguez, D. Ceballos, J. Fores, and X. Navarro. Alignment of collagen and laminin-containing gels improve nerve regeneration within silicone tubes. *Restor. Neurol. Neurosci*. 20:169–179, 2002.

[36]Weiss, P. Experiments of cell and axon orientation in vitro: the role of colliodal exudates in tissue organization. *J. Exp. Zool*. 401–450, 1945.

[37]Whitworth, I. H., R. A. Brown, C. Dore, C. J. Green, and G. Terenghi. Orientated mats of fibronectin as a conduit material for use in peripheral nerve repair. *J. Hand Surg. [Br.]* 20:429–436, 1995.

[38]Williams, L. R., F. M. Longo, H. C. Powell, G. Lundborg, and S. Varon. Spatial-temporal progress of peripheral nerve regeneration within a silicone chamber: Parameters for a bioassay. *J. Comp. Neurol*. 218:460–470, 1983.